

eScholarship@UMassChan

Distinct adipocyte progenitor cells are associated with regional phenotypes of perivascular aortic fat in mice

Item Type	Journal Article
Authors	Tran, Khanh-Van;Fitzgibbons, Timothy P;Min, So Yun;DeSouza, Tiffany;Corvera, Silvia
Citation	<p><p>Mol Metab. 2018 Mar;9:199-206. doi: 10.1016/j.molmet.2017.12.014. Epub 2018 Jan 10. Link to article on publisher's site</p></p>
DOI	10.1016/j.molmet.2017.12.014
Rights	Copyright 2018 The Authors. Open Access funded by National Institutes of Health. This is an open access article under the CC BY-NC-ND license (http://creativecommons.org/licenses/by-nc-nd/4.0/).
Download date	2026-05-21 17:09:28
Item License	http://creativecommons.org/licenses/by-nc-nd/4.0/
Link to Item	https://hdl.handle.net/20.500.14038/29241

Distinct adipocyte progenitor cells are associated with regional phenotypes of perivascular aortic fat in mice



Khanh-Van Tran^{1,2,*,3}, Timothy Fitzgibbons^{1,2,3}, So Yun Min¹, Tiffany DeSouza¹, Silvia Corvera¹

ABSTRACT

Objective: Perivascular adipose tissue depots around the aorta are regionally distinct and have specific functional properties. Thoracic aorta perivascular adipose tissue (tPVAT) expresses higher levels of thermogenic genes and lower levels of inflammatory genes than abdominal aorta perivascular adipose tissue (aPVAT). It is not known whether this distinction is due to the *in-vivo* functional environment or to cell-autonomous traits that persist outside the *in-vivo* setting. In this study, we asked whether the progenitor cells in tPVAT and aPVAT have cell-autonomous traits that lead to formation of regionally distinct PVAT.

Methods: We performed microarray analysis of thoracic and abdominal peri-aortic adipose tissues of C57Bl/6J mice to define gene expression profile of each depot. To derive adipocyte progenitor cells, C57Bl/6J mice were sacrificed and thoracic and abdominal aorta fragments were embedded in Matrigel and cultured under pro-angiogenic conditions. Adipogenesis was induced using the *Ppar-γ* agonist rosiglitazone, a thiazolidinedione (TZD). TZD-induced adipocyte populations were analyzed using immunofluorescence and qRT-PCR.

Results: Microarray analysis showed that tPVAT expressed higher levels of transcription factors related brown adipose tissue development compared to aPVAT. Classic brown adipose tissue (BAT) genes such as *Ucp-1*, *Prdm16*, *Dio2*, *Slc27a* displayed a concordant trend of higher level expression in tPVAT, while white adipose tissue (WAT) genes such as *Hoxc8*, *Nnat*, *Sncg*, and *Mest* were expressed at a higher level in aPVAT. The adipokines resistin and retinol binding protein 4 were also higher in aPVAT. Furthermore, adipocyte progenitors from abdominal and thoracic aortic rings responded to TZD with expression of canonical adipocyte genes *Acrp30*, *Plin1*, and *Glut4*. Adipocytes differentiated from thoracic aorta progenitors displayed markedly higher induction of *Ucp-1* and *Cidea*.

Conclusions: Thoracic aorta PVAT expresses higher levels of brown adipocyte transcription factors than aPVAT. Precursor cells from the thoracic aorta give rise to adipocytes that express significantly higher levels of *Ucp-1* and *Cidea ex vivo*, suggesting that progenitor cells in tPVAT and aPVAT have cell-autonomous properties that dictate adipocyte phenotype.

© 2018 The Authors. Published by Elsevier GmbH. This is an open access article under the CC BY-NC-ND license (<http://creativecommons.org/licenses/by-nc-nd/4.0/>).

Keywords Perivascular adipose tissue; Adipocyte precursors; Progenitors; *Ucp-1*; Adipogenesis; Aorta

1. INTRODUCTION

Perivascular adipose tissue (PVAT) is a newly recognized adipose depot with highly active endocrine and paracrine functions. PVAT secretes a multitude of adipokines and other factors that have important physiological and pathophysiological implications for the adjacent blood vessels [1–6]. Recent studies show that murine thoracic PVAT produces numerous factors, including adiponectin, leptin, H₂S, and other unidentified factors, collectively referred to as adipocyte-derived relaxing factors, that influence vascular function [7–13]. These secreted factors can facilitate a vasodilatory effect through an endothelium-dependent mechanism via nitric oxide (NO) synthesis and

release or an endothelium-independent mechanism via the generation of hydrogen peroxide [10,14]. On the other hand, in obese humans or mice, PVAT has been shown to release factors to promote inflammation, vasoconstriction, or vascular smooth muscle cell proliferation that are detrimental to vascular function [15,16]. Therefore, the physiological importance of PVAT in vascular homeostasis is undisputed and is an area of intense investigation.

Among the most studied murine PVAT is adipose tissue surrounding the aorta. Along the aorta, the phenotype of the PVAT is unique depending on anatomical location [17]. The levels of inflammatory genes and markers of immune cell infiltration are greater in aPVAT than in tPVAT [18]. The aPVAT phenotype is more pro-inflammatory

¹Program in Molecular Medicine, University of Massachusetts Medical School, Worcester, MA, 01655, USA ²Department of Medicine, University of Massachusetts Medical School, Worcester, MA, 01655, USA

³ Khanh-Van Tran and Timothy Fitzgibbons contributed equally to this work.

*Corresponding author. University of Massachusetts Medical School, 368 Plantation Street, AS7-1018, Worcester, MA, 01605, USA.

E-mails: Khanh-van.tran@umassmemorial.org (K.-V. Tran), Timothy.Fitzgibbons@umassmemorial.org (T. Fitzgibbons), ssso1019@hanmail.net (S.Y. Min), Tiffany.DeSouza@umassmed.edu (T. DeSouza), Silvia.Corvera@umassmed.edu (S. Corvera).

Received November 26, 2017 • Revision received December 18, 2017 • Accepted December 24, 2017 • Available online 10 January 2018

<https://doi.org/10.1016/j.molmet.2017.12.014>

and atherogenic than the tPVAT phenotype and may explain why aneurysms more frequently occur in the abdominal aorta [17–19]. PVAT surrounding the murine thoracic aorta (tPVAT) exhibits phenotypic features of brown adipose tissue (BAT), and that surrounding the abdominal aorta PVAT (aPVAT) is more similar to white adipose tissue (WAT) [17–19]. White adipose tissue (WAT) classically functions to store excess energy in the form of triglyceride. In contrast, brown adipose tissue (BAT) oxidizes fatty acids to generate heat. “Beige” adipocyte exists in WAT and can be induced by cyclic adenosine monophosphate (cAMP) to express thermogenic genes to resemble BAT [20]. Although it is clear that there are inherent phenotypic differences between tPVAT and aPVAT, it is unclear whether these differences are the result of extrinsic anatomical factors or intrinsic cell autonomic properties. For example, higher beta-adrenergic signaling could induce expression of brown adipocyte genes even if precursors cells are inherently the same existing in different environments [21]. In contrast, the cells could be intrinsically different due to transcriptional programming and would develop into distinct adipocyte in an environment-independent manner.

In this study, we sought to answer this question by analyzing transcriptomic data from peri-aortic adipose tissue and studying progenitor cells that give rise to new adipocytes from different regions of mouse aorta. For this purpose, we used the traditional *ex vivo* aortic ring assay to study progenitor cells arising from thoracic and abdominal aortic regions. Originally, Nicosia and Ottinetti designed the *ex vivo* aortic ring assay to study angiogenesis [22]. Cells arising from aortic rings form tubular structures and lumenize. Since its first introduction, this method has been widely used to study angiogenesis. Adipocyte progenitor cells are known to reside in the vasculature of the adipose tissue [23–26]. The vasculature, such as the aorta, harbors PVAT progenitor cells. As such, we used the peroxisome proliferator-activated receptor gamma (*Ppar-γ*) agonist Rosiglitazone, a thiazolidinedione (TZD), to stimulate adipogenesis in precursor cells emerging from aortic explants from thoracic and abdominal aortic rings. We observed that cells emerging from the aortic ring take on adipocyte morphology, express adipocyte markers, and secrete adiponectin. Furthermore, we found that TZD-induced tPVAT expresses higher levels of hallmark brown adipocyte genes, uncoupling protein 1 (*Ucp-1*) and cell death activator CIDE-A (*Cidea*), than aPVAT. Our microarray analysis showed that transcription factors relating to brown adipocyte development are elevated in tPVAT compared to aPVAT. Taken together, our results demonstrate that preadipocytes residing in tPVAT and aPVAT have cell-autonomous characteristics that dictate phenotypic development.

2. MATERIAL AND METHODS

2.1. Microarray analysis

All animal experiments in this work has been approved by the Institutional Animal Care and Use Committee of University of Massachusetts Medical School. Briefly, C57Bl/6J mice were sacrificed using CO₂ and cervical dislocation. The heart and vasculature were flushed with PBS. Thoracic PVAT directly adjacent to the lesser curvature of the aortic arch and aPVAT from above the renal arteries to the diaphragm were harvested and snap frozen in liquid nitrogen. RNA was isolated from thoracic and abdominal PVAT as previously described [19]. RNA concentrations were determined using a Nanodrop 2000 Spectrophotometer (Thermo Fisher, Wilmington, DE). The RNA quality was assessed using an Agilent 2100 Bioanalyzer (Agilent Technologies, Santa Clara, CA). Only samples with a RNA integrity number 7.5 and

normal 18- and 28-s fractions on microfluidic electrophoresis were used. RNA from two mice per tissue and diet was pooled for a total of 250 ng total RNA template for cDNA synthesis and in vitro transcription using the Ambion WT expression kit (Ambion, Carlsbad, CA). Second-strand cDNA was then labeled with the Affymetrix WT terminal labeling kit, and samples were hybridized to Affymetrix Mouse Gene 1.0 ST arrays (Affymetrix, Santa Clara, CA). Gene chip expression array analysis for individual genes was performed as previously described, filtering for $p < 0.05$. Three biological replicate hybridizations per tissue were performed, for a total of 6 hybridizations. We analyzed microarray data using Affymetrix Transcriptome Analysis Console (TAC) Software, which integrates *limma*, a core component of Bioconductor project using the statistical computing language R [27]. Pathway analysis of transcriptomic data was performed using Broad Institute Molecular Signature Database: Hallmark Gene Set and well as Qiagen’s Ingenuity® Pathway Analysis, with genes with $p < 0.05$ and a fold change of 2.

2.2. Aortic ring assay

C57Bl/6J mice were sacrificed as above. After cutting side branches throughout, the aorta was excised from the root to the femoral bifurcation. PVAT was removed under a dissecting microscope leaving the tunica externa intact. The thoracic aorta was determined to be segments from the aortic arch to the diaphragm and the abdominal aorta was determined to be segments from below the diaphragm to femoral bifurcation. The aortic fragments were washed with EGM-2 media and cut into 1 mm ring segments. Each aortic ring segment was embedded in a singular well of a 96-well plate containing 40 μ L of Matrigel (BD Discovery Labware). After aorta was embedded in the 96-well plate, the plate was allowed to stand for 30 min in the 37 °C so that the Matrigel would solidify. The cells were fed with 200 μ L of EGM-2 media, which was changed every other day. The mouse aorta fragments were mechanically excised, and the endothelial sprouts remaining in the Matrigel were isolated using Dispase II (Roche, 2.4 U/mL), centrifuged, and RNA extracted from the pellet using an Ambion RNA extraction kit. Probes used are specified in Table 5 of Appendix.

2.3. Staining and analysis

Pieces of aortic rings were embedded in Growth Factor Reduced Matrigel (BD Biosciences) in 35 mm glass-bottom culture dishes (MatTek Corporation), and cultured in EGM-2 media for 14 days. After 14 days in culture with and without rosiglitazone, explants were fixed in 4% Formaldehyde (Ted Pella, Inc.) in PBS for 15 min and permeabilized in 0.5% TX-100 in PBS for 30 min. The primary antibodies used to characterize the origin of cells growing from the explants were mouse Cd31 (BD Pharmingen, clone MEC 13.3, 1:50), mouse Cd34 (BD Pharmingen, clone RAM34, 1:50), monoclonal mouse Adiponectin (Peirce, PA1-054, 1:200), and polyclonal Guinea Pig Perilipin (Fitzgerald Industries International, 20R-PP004, 1:200). Secondary antibodies were species matched Alexa Fluor 594, and Alexa Fluor 488 (Molecular probes, 1:500). Negative controls treated with irrelevant mouse IgG instead of primary antibody were processed simultaneously. All sections were counterstained with DAPI (Molecular Probes).

2.4. Western blotting

The mouse aorta fragments were mechanically excised and the sprouts remaining in the Matrigel were isolated using Dispase II (Roche, 2.4 U/mL). Cell lysates were prepared using the Complete

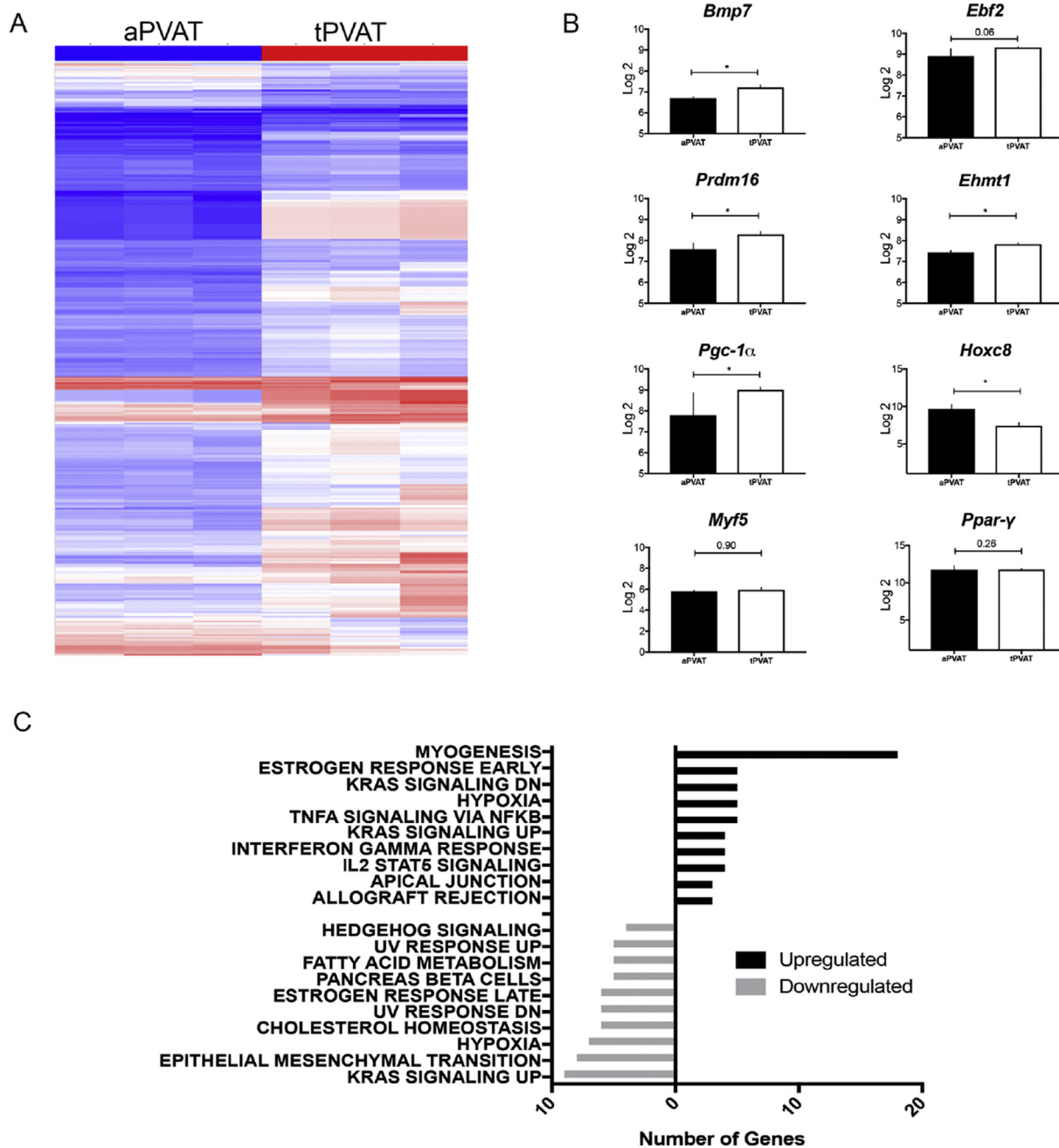


Figure 1: Differential gene expression in tPVAT and aPVAT (A) Hierarchical cluster analysis (HCA) of aPVAT and tPVAT demonstrates that PVAT differs by anatomic location. (B) Transcription factors involved in brown fat adipogenesis *Prdm16*, *Ehmt1*, *Bmp7*, *Ebf2*, and *Pgc-1 α* are upregulated in tPVAT as compared to aPVAT. *Myf5* and *Ppar- γ* were not upregulated in tPVAT, and *Hoxc8* was downregulated in tPVAT compared to aPVAT (C) Pathway analysis of transcriptomic data using the Broad Institute Molecular Signature Database: Hallmark Gene Set. Statistical analysis was performed using one-way ANOVA test within Affymetrix Transcriptome Analysis Console (TAC) Software: *p value < 0.05.

Lysis-M kit (Roche). Protein concentration was measured using the Beckman DU-640B Spectrophotometer. Equal amounts of protein (20 μ g) and conditioned media (40 μ l) were loaded and analyzed by western blot in accordance with standard procedure. The primary antibodies used were polyclonal Guinea Pig Perilipin (Fitzgerald Industries International, 20R-PP004, 1:2000) and goat polyclonal to beta actin (Abcam, ab8229, 1:5000) for cell lysate and rabbit polyclonal anti-Adiponectin (Pierce, PA1-054, 1:10000) for media. The secondary antibodies were goat anti-rabbit (Promega), rabbit anti-goat (Abcam), and goat anti-guinea pig antibody (Millipore).

3. RESULTS

It was previously reported that tPVAT resembles BAT and aPVAT resembles more of WAT [17–19]. To understand the mechanism by which they differ in phenotype, we performed transcriptome analysis of both tissues. Unsupervised hierarchical clustering analysis (HCA) demonstrated that tPVAT and aPVAT clustered based on anatomical location (Figure 1). Consistent with results previously described, microarray analysis showed that tPVAT has a gene expression profile resembling BAT. Thoracic aortic PVAT trended to express classical BAT

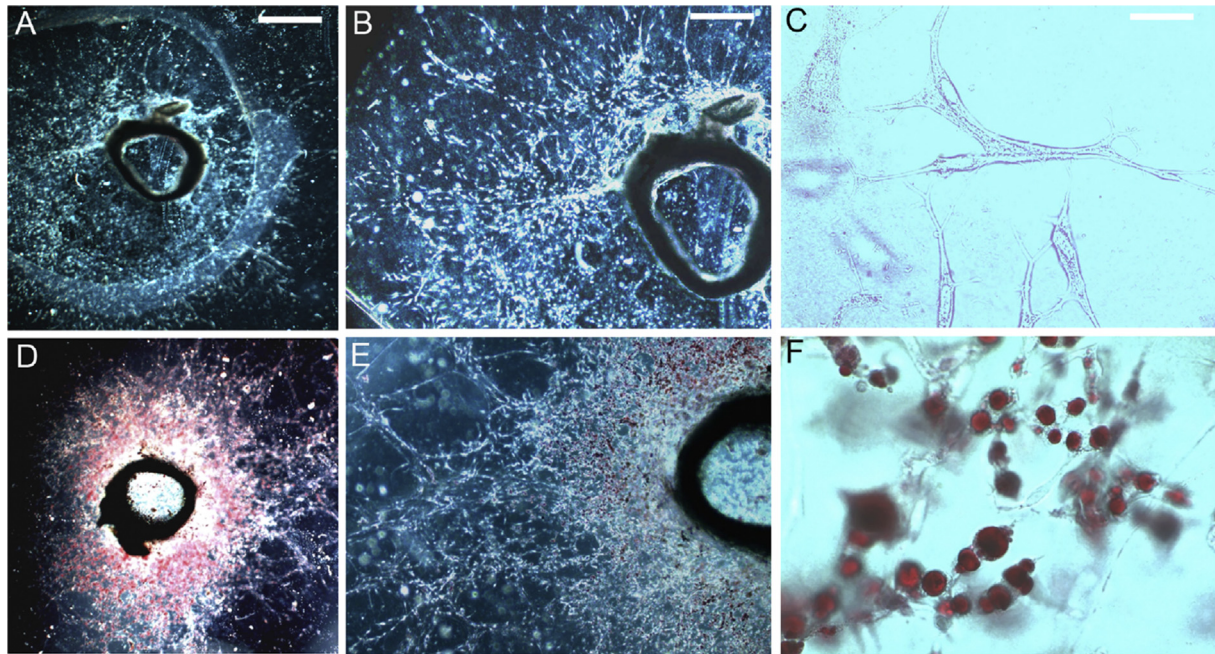


Figure 2: Oil-Red-O staining of cells arising from the thoracic aorta in the presence of TZD (Rosiglitazone). Representative photomicrographs of capillary sprouts growing from thoracic aorta explants in the absence (A, B, and C) and in the presence of TZD (D, E and F) stained with Oil-Red-O for identification of lipid droplets. Positive Oil-Red-O staining is observed only in the presence of TZD. Scale bars are 1000 μm , 500 μm and 100 μm , respectively.

genes such as *Ucp-1*, PR domain containing 16 (*Prdm16*), deiodinase (*Dio2*), fatty acid transporter (*Slc27a*) at higher levels than aPVAT (Supplementary Table 1). Quantitative RT-PCR confirmed that tPVAT expressed *Ucp-1* at a higher level than aPVAT (Supplementary Figure 1). Abdominal PVAT expressed highly enriched WAT genes such as *Hoxc8*, *Nnat*, *Sncg* and *Mest*. Expression of the adipokines, resistin (*Retn*) and retinol binding protein 4 (*Rbp4*), were also higher in aPVAT. Interestingly, among the most upregulated genes in tPVAT compared to aPVAT were genes associated with muscle structure and function such as actin, myosin and troponin (Supplementary Table 1).

Gene set enrichment analysis (GSEA) revealed that expression of genes regulating myogenesis was the most upregulated pathway in tPVAT. Cholesterol homeostasis and well as fatty acid metabolism were among downregulated pathways in tPVAT compared to aPVAT (Figure 1). Microarray analysis of tPVAT and aPVAT also revealed that several transcription factors involved in the development of brown adipocytes from precursor cells such as bone morphogenetic protein 7 (*Bmp7*), early B-Cell factor 2 (*Ebf2*), euchromatic histone-lysine N-methyltransferase 1 (*Ehmt1*), *Prdm16* and peroxisome proliferator-activated receptor-gamma coactivator 1 alpha (*PGC-1 α*) were expressed at a higher level in tPVAT compared to aPVAT (Figure 1.) Interestingly, myogenic factor 5 (*Myf5*), a gene involved in the lineage of muscle and brown adipocyte, and *Ppar- γ* were not significantly elevated in the tPVAT compared to aPVAT. Increased expression of the transcription factors relating to brown adipocyte development suggest differences in progenitor cells residing in tPVAT and aPVAT.

As microarray data show that transcription factors involved in the development of brown adipocytes were upregulated in tPVAT compared to aPVAT, we investigated perivascular adipose progenitor cells residing in the mouse aorta. Previous studies have shown that progenitor cells reside in the vasculature of the adipose tissue [23–26]. As such, we embedded thoracic aortic rings devoid of PVAT in Matrigel and treated them with the TZD rosiglitazone, a PPAR- γ

agonist, to induce adipocyte formation. We found that in the presence of TZD, cells arising from the aortic rings can accumulate lipid droplets (Figure 2). The morphology of cells is no longer spindle-like, rather they resemble multilocular fat cells. Oil-Red-O staining clearly identified lipid droplets in cells coming from the aorta.

To confirm that these cells are adipocytes accumulating lipid droplets, we used immunofluorescence and real-time PCR to confirm expression of adipocyte genes. We found that after 14 days in the presence of TZD, expression of the endothelial specific genes *Cd31* and *Cd34* is decreased (Figure 3). Conversely, expression of the adipocyte specific genes adiponectin (*Acrp30*) and perilipin (*Plin1*) are increased. In particular, the pattern of expression of the *Plin1* in these cells is consistent with an adipocyte identity. Approximately 20% of cells differentiated into adipocytes, as assessed by presence of *Plin1* relative to Dapi (data not shown). Quantitative PCR also demonstrated a decrease in the endothelial specific markers, *Cdh5* and *Cd34*, and an increase in the adipocyte markers, *Acrp30*, *Glut4*, *Cidea*, and *Ucp-1* (Figure 3). We further tested conditioned media of sprouts growing from aorta explants for the secretion of *Acrp30*. We confirmed that these TZD-induced fat cells are secreting *Acrp30*, a canonical adipokine, after approximately 13 days in culture (Figure 3).

After successfully inducing perivascular adipocyte formation in *ex vivo* aortic rings, we used our model to compare adipocyte progenitor cells from tPVAT and aPVAT. We examined the growth of capillary sprouts from the thoracic and abdominal regions of aorta (Figure 4). TZD increased the expression of *Acrp30*, *Glut4*, *Plin1*, *Cidea*, and *Ucp-1* in cells arising from the abdominal and thoracic aortic rings. Interestingly, *Acrp30*, *Glut4*, and *Plin1* were not differentially expressed in cells arising from aPVAT and tPVAT explants. However, TZD-induced adipocytes arising from the thoracic aorta had much higher expression of both *Cidea* and *Ucp-1* (Figure 4), hallmark brown adipocyte genes. The levels of *Ucp-1* and *Cidea* expression in TZD-induced adipocytes was not as high as that in interscapular BAT (Figure 4).

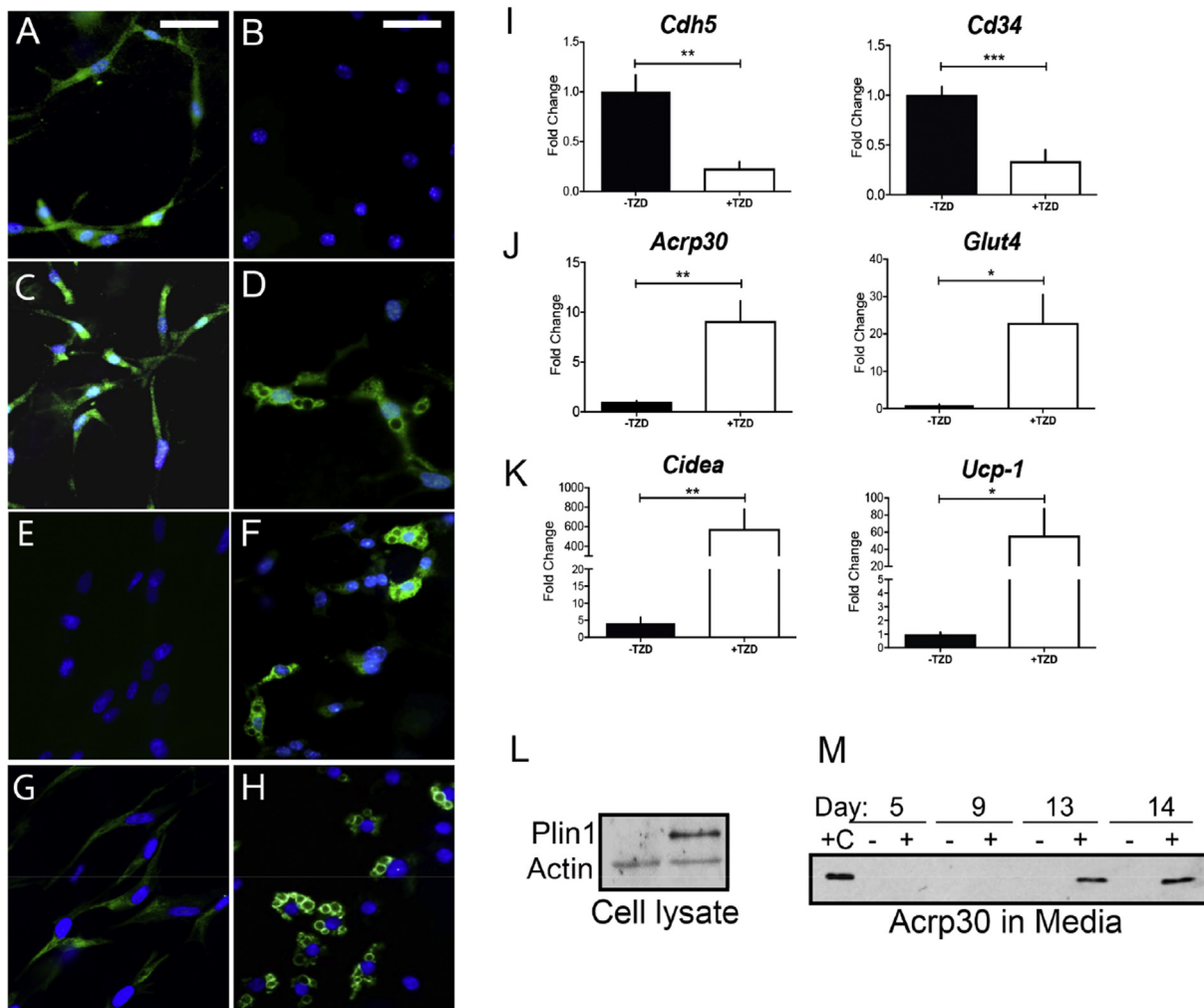


Figure 3: TZD-induced adipocyte formation from mouse thoracic aortic ring. In the absence of TZD (A, C, E and G), cells arising from thoracic aortic rings are positive for Cd31 (A) and Cd34 (B), but are negative for Acrp30 (E) and Plin1 (G). In the presence of TZD (B, D, F, and H), expression of Cd31 and Cd34 (B and D) are altered, and there is an increase in the expression of Acrp30 and Plin1 (F and H). Furthermore, mRNA levels of cells arising from aortic rings at day 14 in culture in the absence and presence of TZD were assessed (I–K.) There is a significant decrease in *Cdh5* and *Cd34* and an increase in *Acrp30*, *Glut4*, *Cidea*, and *Ucp-1*. Western blot (L) analysis of Plin1 in capillary sprouts growing from aorta explants in the absence and presence of TZD. TZD induced expression of Plin1 in the cell lysates, as well, as secretion of Acrp30 (M) into the media. Normal mouse serum was used as a positive control for Acrp30 detection. Scale bar is 100 μ m. Statistical analysis was performed using unpaired Student t-test: * $p < 0.05$, ** $p < 0.005$, *** $p < 0.0005$.

4. DISCUSSION

Our transcriptome analysis of tPVAT and aPVAT suggests that progenitors in tPVAT are transcriptionally primed to develop into brown adipocytes. In previous work, *Ebf2* was found to be selectively expressed in brown preadipocytes. When ectopically expressed in myoblasts or white preadipocytes, *Ebf2* recruited *Ppar- γ* to brown-selective binding sites and reprogrammed cells to a brown adipocyte fate [28]. Furthermore, Tseng and colleagues have found that *Bmp7* activates a full program of brown adipogenesis including induction of early regulators of brown adipocyte fate such as *Prdm16* and *Pgc-1 α* [29]. *Ehmt1* complexes with *Prdm16* to activate the brown adipocyte transcriptional program [30]. In our analysis, expression of *Prdm16*, *Ehmt1*, *Bmp7*, and *Pgc-1 α* were all significantly upregulated in tPVAT compared to aPVAT; and there was a non-significant trend for increased *Ebf2* expression in tPVAT. *Hoxc8*, which is a homeobox gene thought to target and repress CCAAT/enhancer binding protein beta, a

master regulator of the brown-adipocyte gene program, is increased in aPVAT compared to tPVAT [31]. In summary, many of the transcription factors that have been implicated in brown adipocyte formation are upregulated in tPVAT compared to aPVAT. Our results suggest that the adipocyte precursor cells that reside in the thoracic and aorta are distinct and have cell-autonomous traits that dictate adipocyte phenotype.

Pathway analysis of the transcriptome data using the Broad Institute Molecular Signature Database: Hallmark Gene Set showed that the myogenesis pathway is most upregulated pathway in tPVAT compared to aPVAT (Figure 1). Furthermore, genes relating to skeletal and smooth muscle structure and function among the genes that are most upregulated (Supplementary Table 3 and Figure 2). Fitzgibbons and colleagues have found that genes of skeletal muscle function are higher in BAT than tPVAT [19]. Timmons et al. have also found a number of muscle related genes that are expressed in BAT [32]. Brown adipocyte precursors are thought to share a common ancestor with skeletal

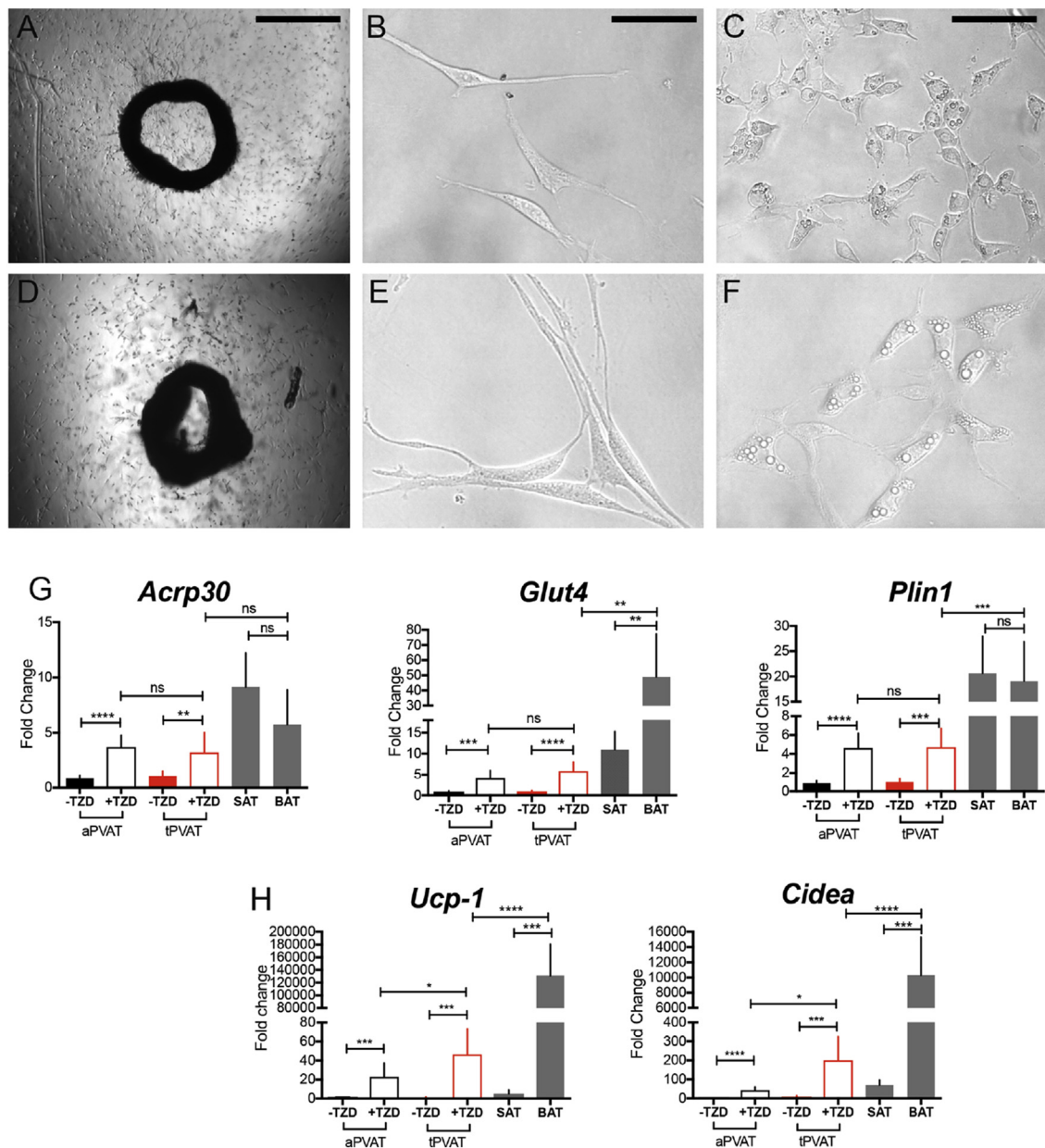


Figure 4: Capillary sprouts arise from both abdominal and thoracic aorta fragments give rise to distinct adipocytes. Cells arising from thoracic (A-C) and abdominal (D-F) rings were analyzed in the absence (B and E), and in the presence of TZD (C and F). TZD induced the formation of multicellular adipocytes from both segments of aorta. TZD increased the expression of *Acrp30*, *Glut4*, *Plin1*, *Ucp-1*, and *Cidea* in cells arising from the aorta (G and H). However, the up-regulation of *Ucp-1* and *Cidea* in cells from the thoracic aortic region was much higher than that observed in cells from the abdominal aortic region (H). Subcutaneous inguinal WAT (SAT) and intrascapular BAT (BAT) were used as controls. Scale bars are 1000 μ m and 100 μ m, respectively. Statistical analysis was performed using unpaired Student t-test: * $p < 0.05$, ** $p < 0.005$, *** $p < 0.0005$, **** $p < 0.00005$.

muscle cell that express *Myf5* [33]. Alternatively, beige adipocyte precursors are thought to be distinct from brown adipocyte precursors, in that they derive from a non-*Myf5* expressing cells of smooth muscle origin [34]. Chang et al. demonstrated that mice with conditional knockout of *Ppar- γ* in smooth muscle cells are devoid of PVAT, suggesting that PVAT is derived from a smooth muscle cell origin [35]. In our prior microarray analysis, expression of the beige cell specific gene *Slc27a1* tended to be higher in tPVAT than BAT, but not significantly [19]. In our current analysis, the muscle related genes upregulated included that of smooth and skeletal muscle (Supplementary Figure 2

and Table 3). Therefore, the precise origin of tPVAT is controversial and remains to be determined. Nonetheless, our transcriptome analysis suggests that the progenitor cells in tPVAT are transcriptionally activated to take on a “browner” phenotype in comparison to aPVAT. We induced formation of adipocytes from the thoracic and abdominal aortic rings of mice to further study adipose progenitor cells from different areas of the aorta. We found that progenitor cells from each area of the aorta give rise to distinct adipocytes even when removed from the *in vivo* environment. Preadipocytes from thoracic aortic rings give rise to adipocytes that express higher levels of *Ucp-1* and *Cidea*,

BAT specific genes. TZDs are known to induce *Ucp-1* expression, but the induction is much higher in the tPVAT compared to aPVAT [36]. Results from our *ex vivo* aortic ring experiment support the hypothesis that progenitor cells from thoracic and abdominal aorta have cell-autonomous trait that dictate their development into distinct adipocytes. The progenitor cells maintain their inherent identity even when removed from their *in vivo* environment. This distinction in their identity is supported by our microarray data which shows upregulation of BAT specific transcription factors expression in tPVAT compared to aPVAT. Although the aortic ring assay is widely used to study angiogenesis, this the first time that it has been used to study PVAT. Angiogenesis and adipogenesis are closely related *in vivo* [37]. This model allows the cross talk between endothelial cells and adipocytes to be maintained. We found that expression of endothelial cells specific genes was decreased, and adipocyte specific gene expression was increased upon stimulation with TZD. This likely reflects TZD favoring the adipocyte progenitor cells to differentiate and proliferate. The limitations to this system is that it is technically difficult to remove all adipose tissue from the mouse aorta. Thus, it is not completely clear if progenitor cells are arising from adipose tissue depots or from the aorta per-se. Nevertheless, the aortic ring assay is a useful model to study the development and characteristics of PVAT.

Understanding the identity of the PVAT progenitors and the adipocytes they give rise to is key for manipulation of the adipocyte phenotype to improve metabolic and vascular health. Ohman et al. have shown visceral adipose tissue transplantation to the carotid artery in mouse lead to endothelial cell dysfunction and accelerated atherosclerosis compared to subcutaneous adipose transplantation. Furthermore, disruption of PVAT formation disturbs intravascular thermoregulation in mice and lead to increased atherosclerosis [35,38]. In humans, gene expression profile of PVAT surrounding coronary artery (PVAT-CA) and PVAT surrounding the internal thoracic arteries (PVAT-IMA) are unique [39]. Interestingly, patients with coronary artery disease have upregulation of inflammatory and lipid metabolism pathways in gene expression patterns of PVAT-CA compared to PVAT-IMA, implicating adipose tissue inflammation and lipid metabolism as key factors in the development of atherosclerosis [39]. Thus, studying the various phenotypes of PVAT is critical for the understanding and treatment of vascular disease, such as atherosclerosis.

In conclusion, we used transcriptome analysis and the aortic ring assay to show that progenitor cells from tPVAT are transcriptionally primed to develop into more thermogenic adipocyte in comparison with aPVAT. Our study highlights the phenotypic differences between progenitors of aPVAT and tPVAT. To the best of our knowledge, this is the first time the aortic ring assay has been used to study perivascular adipose tissue and their progenitors.

ACKNOWLEDGMENT

This work was funded in part by NIH grant DK089101 to Dr. Silvia Corvera and AHA grant #12FTF11260010 to Dr. Timothy Fitzgibbons.

CONFLICT OF INTEREST

None declared.

APPENDIX A. SUPPLEMENTARY DATA

Supplementary data related to this article can be found at <https://doi.org/10.1016/j.molmet.2017.12.014>.

REFERENCES

- [1] Montero, D., et al., 2012. Endothelial dysfunction, inflammation, and oxidative stress in obese children and adolescents: markers and effect of lifestyle intervention. *Obesity Reviews* 13(5):441–455.
- [2] Lau, D.C., et al., 2005. Adipokines: molecular links between obesity and atherosclerosis. *American Journal of Physiology - Heart and Circulatory Physiology* 288(5):H2031–H2041.
- [3] Knudson, J.D., et al., 2008. Leptin and mechanisms of endothelial dysfunction and cardiovascular disease. *Current Hypertension Reports* 10(6):434–439.
- [4] Li, F.Y., et al., 2011. Cross-talk between adipose tissue and vasculature: role of adiponectin. *Acta Physiologica* 203(1):167–180.
- [5] Ronti, T., et al., 2006. The endocrine function of adipose tissue: an update. *Clinical Endocrinology* 64(4):355–365.
- [6] Szasz, T., Webb, R.C., 2012. Perivascular adipose tissue: more than just structural support. *Clinical Science* 122(1):1–12.
- [7] Schleifenbaum, J., et al., 2010. Systemic peripheral artery relaxation by KCNQ channel openers and hydrogen sulfide. *Journal of Hypertension* 28(9): 1875–1882.
- [8] Oriowo, M.A., 2015. Perivascular adipose tissue, vascular reactivity and hypertension. *Medical Principles and Practice* 24(Suppl 1):29–37.
- [9] Lee, R.M., et al., 2009. Endothelium-dependent relaxation factor released by perivascular adipose tissue. *Journal of Hypertension* 27(4):782–790.
- [10] Galvez-Prieto, B., et al., 2012. Anticontractile effect of perivascular adipose tissue and leptin are reduced in hypertension. *Frontiers in Pharmacology* 3:103.
- [11] Fesus, G., et al., 2007. Adiponectin is a novel humoral vasodilator. *Cardiovascular Research* 75(4):719–727.
- [12] Fang, L., et al., 2009. Hydrogen sulfide derived from perivascular adipose tissue is a vasodilator. *Journal of Hypertension* 27(11):2174–2185.
- [13] Victorio, J.A., et al., 2016. Different anti-contractile function and nitric oxide production of thoracic and abdominal perivascular adipose tissues. *Frontiers in Physiology* 7:295.
- [14] Gao, Y.J., et al., 2007. Modulation of vascular function by perivascular adipose tissue: the role of endothelium and hydrogen peroxide. *British Journal of Pharmacology* 151(3):323–331.
- [15] Ozen, G., et al., 2015. Human perivascular adipose tissue dysfunction as a cause of vascular disease: focus on vascular tone and wall remodeling. *European Journal of Pharmacology* 766:16–24.
- [16] Maenhaut, N., Van de Voorde, J., 2011. Regulation of vascular tone by adipocytes. *BMC Medicine* 9:25.
- [17] Padilla, J., et al., 2013. Divergent phenotype of rat thoracic and abdominal perivascular adipose tissues. *American Journal of Physiology - Regulatory, Integrative and Comparative Physiology* 304(7):R543–R552.
- [18] Police, S.B., et al., 2009. Obesity promotes inflammation in periaortic adipose tissue and angiotensin II-induced abdominal aortic aneurysm formation. *Arteriosclerosis, Thrombosis, and Vascular Biology* 29(10):1458–1464.
- [19] Fitzgibbons, T.P., et al., 2011. Similarity of mouse perivascular and brown adipose tissues and their resistance to diet-induced inflammation. *American Journal of Physiology - Heart and Circulatory Physiology* 301(4):H1425–H1437.
- [20] Petrovic, N., et al., 2010. Chronic peroxisome proliferator-activated receptor gamma (PPARGgamma) activation of epididymally derived white adipocyte cultures reveals a population of thermogenically competent, UCP1-containing adipocytes molecularly distinct from classic brown adipocytes. *Journal of Biological Chemistry* 285(10):7153–7164.
- [21] Collins, S., et al., 2010. Positive and negative control of *Ucp1* gene transcription and the role of beta-adrenergic signaling networks. *International Journal of Obesity* 34(Suppl 1):S28–S33.
- [22] Nicosia, R.F., Ottinetti, A., 1990. Growth of microvessels in serum-free matrix culture of rat aorta. A quantitative assay of angiogenesis in vitro. *Laboratory Investigation* 63(1):115–122.

Brief Communication

- [23] Tang, W., et al., 2008. White fat progenitor cells reside in the adipose vasculature. *Science* 322(5901):583–586.
- [24] Tran, K.V., et al., 2012. The vascular endothelium of the adipose tissue gives rise to both white and brown fat cells. *Cell Metabolism* 15(2):222–229.
- [25] Gupta, R.K., et al., 2012. Zfp423 expression identifies committed pre-adipocytes and localizes to adipose endothelial and perivascular cells. *Cell Metabolism* 15(2):230–239.
- [26] Berry, R., Rodeheffer, M.S., 2013. Characterization of the adipocyte cellular lineage in vivo. *Nature Cell Biology* 15(3):302–308.
- [27] Ritchie, M.E., et al., 2015. Limma powers differential expression analyses for RNA-sequencing and microarray studies. *Nucleic Acids Research* 43(7):e47.
- [28] Rajakumari, S., et al., 2013. EBF2 determines and maintains brown adipocyte identity. *Cell Metabolism* 17(4):562–574.
- [29] Tseng, Y.H., et al., 2008. New role of bone morphogenetic protein 7 in brown adipogenesis and energy expenditure. *Nature* 454(7207):1000–1004.
- [30] Ohno, H., et al., 2013. EHMT1 controls brown adipose cell fate and thermogenesis through the PRDM16 complex. *Nature* 504(7478):163–167.
- [31] Mori, M., et al., 2012. Essential role for miR-196a in brown adipogenesis of white fat progenitor cells. *PLoS Biology* 10(4):e1001314.
- [32] Timmons, J.A., et al., 2007. Myogenic gene expression signature establishes that brown and white adipocytes originate from distinct cell lineages. *Proceedings of the National Academy of Sciences of the United States of America* 104(11):4401–4406.
- [33] Seale, P., et al., 2008. PRDM16 controls a brown fat/skeletal muscle switch. *Nature* 454(7207):961–967.
- [34] Long, J.Z., et al., 2014. A smooth muscle-like origin for beige adipocytes. *Cell Metabolism* 19(5):810–820.
- [35] Chang, L., et al., 2012. Loss of perivascular adipose tissue on peroxisome proliferator-activated receptor-gamma deletion in smooth muscle cells impairs intravascular thermoregulation and enhances atherosclerosis. *Circulation* 126(9):1067–1078.
- [36] Coelho, M.S., et al., 2016. GQ-16, a TZD-derived partial PPARgamma agonist, induces the expression of thermogenesis-related genes in Brown fat and visceral white fat and decreases visceral adiposity in obese and hyperglycemic mice. *PLoS One* 11(5):e0154310.
- [37] Han, J., et al., 2011. The spatiotemporal development of adipose tissue. *Development* 138(22):5027–5037.
- [38] Ohman, M.K., et al., 2011. Perivascular visceral adipose tissue induces atherosclerosis in apolipoprotein E deficient mice. *Atherosclerosis* 219(1):33–39.
- [39] Lu, D., et al., 2017. Gene expression profiling reveals heterogeneity of perivascular adipose tissues surrounding coronary and internal thoracic arteries. *Acta Biochimica et Biophysica Sinica* 49(12):1075–1082.